

The Control of Asymmetric Rolling Missiles Based on Improved Trajectory Linearization Control Method

Huadong Sun¹, Jianqiao Yu¹, Siyu Zhang¹

ABSTRACT: According to motion characteristic of an asymmetric rolling missile with damage fin, a three-channel controlled model is established. The controller which is used to realize non-linear tracking and decoupling control of the roll and angle motion is introduced based on an improved trajectory linearization control method. The improved method is composed of the classic trajectory linearization control method and a compensation control law. The classic trajectory linearization control method is implemented in the time-scale separation principle. The Lipschitz non-linear state observer systematically obtained by solving the linear matrix inequality approach is provided to estimate state variables and unknown parameters, and then the compensation control law utilizing the estimated unknown parameters improves the TLC method. Simulation experiments show that the adaptive decoupling control ensure tracking performance, and the robustness and accuracy of missile attitude control are ensured under the condition of the system parameters uncertainty, random observation noise and external disturbance caused by damage fin.

KEYWORDS: Asymmetric, Rolling missiles, Control, Improved TLC, Lipschitz adaptive observer.

INTRODUCTION

The structure or the aerodynamic asymmetric phenomenon is common for many rolling missiles.

Such unintended asymmetric phenomenon is often caused by two reasons: machining or assembling misalignment and body or fin structural damage by large external forces during the launch or the flight.

Because of uncertainty and random asymmetric factors, the asymmetric rolling missile system is a complex non-linear system with uncertainty parameters. The research on dynamic modeling and control of asymmetric rolling missile is an important problem.

Scholars carried out in-depth research in the dynamic and modeling of asymmetric aircraft. Asymmetric aerodynamic characteristics were the first to be of concern, and wing bending and impact damage were studied by the use of wind tunnel experiments (Render *et al.* 2007; Djellal and Ouibrahim 2008; Render *et al.* 2009). The dynamic problems were also the focus of the study. For an asymmetric rolling missile, when the roll rate nears to the natural frequency of pitch or yaw motion, the roll rate of the missile may be locked and maintained in the natural frequency, and the phenomenon is named lock-in. If the angle of attack of the missile becomes bigger and bigger, the catastrophic yaw happens. Since the lock-in mechanism and the phenomenon of catastrophic yaw were revealed (Murphy 1989), the research about asymmetric rolling missile motion model and dynamic behaviors are widely investigated. By the use of coupling angular motion and roll motion of 5-degrees-of-freedom equations, different dynamic behaviors such as limit

¹Beijing Institute of Technology – School of Aerospace Engineering – Beijing – China.

Author for correspondence: Huadong Sun | Beijing Institute of Technology – School of Aerospace Engineering | Tiyu N Rd, Haidian | Beijing, 10081 – China | Email: huadongsun@163.com

Received: 02/18/2016 | Accepted: 05/09/2016

and chaos of asymmetric rolling missile were studied (Murphy 1989; Ananthkrishnan and Raisinghani 1992; Mikhail 1998; Tanrkulu 1999; Sun *et al.* 2015; Morote 2007; Morote *et al.* 2013). Bifurcation analysis was introduced to investigate the evolutionary process of dynamic behaviors such as lock-in and limit circle in quantitatively and qualitatively ways (Sun *et al.* 2015).

The control method of investigation and controller design are important things for an asymmetric rolling missile. Two types of fin damage were studied in the modeling and missile guidance law designing, and the classical proportional-integral-derivative (PID) control method was used (Harris and Slegers 2009). Research on non-linear control for the uncertainty parameters aircrafts was quite extensive, and it has been a hot issue of scholar's attention. Non-linear controls, such as robust adaptive (Rajagopal *et al.* 2010), sliding mode (Yang *et al.* 2012), and dynamic inversion (Nguyen *et al.* 2006), were applied in the presence of asymmetry of aircraft and spacecraft with uncertainties or other factors. Among these methods, trajectory linearization control (TLC) is a simple but effective gain scheduling means to solve non-linear and uncertainty system. TLC has been successfully applied in missiles (Mickle and Zhu 2001), robots (Liu *et al.* 2003), aircrafts (Zhu and Huizenga 2004), and other objects (Bevacqua *et al.* 2004; Su *et al.* 2013).

However, the control performance of TLC method can significantly be reduced or even infeasible in the presence of serious uncertainties (Zhu and Huizenga 2004). Besides, for most physical missile systems, another major difficulty for TLC are strong external disturbances and model uncertainties due to either constant or sudden changes. TLC faces a big challenge to deal with difficulties of cross coupling, modeling errors, external disturbances, and sensor noise effectively. In addition, the complex dynamic behaviors, such as lock-in, limit circle, and even chaos phenomenon, increase the control difficulty, and furthermore the complexity is exacerbated because of strong cross yaw-roll dynamical coupling caused by the missile rotation. Improving TLC algorithm is an issue of great significance.

This paper aims at designing a good performance control system for asymmetric rolling missiles and developing an improved method for TLC algorithm. Firstly, considering the external force caused by damage fin, a three-channel controlled model for asymmetric rolling missiles is established by the time-scale separation principle. Secondly, control law is presented using improved TLC method in which an adaptive compensation control law is added based on Lipschitz observer.

Lastly, simulation experiments are carried out, and the results show that the performance of three-channel attitude control is well-exhibited. The control effectiveness of the proposed improved method is more robust than TLC.

MOTION MODEL

For an aerodynamic asymmetric cruciform finned missile with fixed rolling rate, the moment equations expressed by the complex angle of attack ξ and the complex angular velocity μ can be given in the aeroballistic axes (Murphy 1963), illustrated in Fig. 1. For a controlled missile with air rudders, compared with the aerodynamic force produced by the body, the air rudder force is a small term. Neglecting the small force produced by the rudder but taking the moment into consideration, the motions can be transformed to the body fix axes and provided as:

$$\xi' = \left[-C_{L\alpha}^* - i\phi'(C_{Np\alpha}^* + 1) \right] \xi + i\gamma\mu \tag{1}$$

$$\begin{aligned} \mu' = & k_t^{-2} (\phi' C_{Mpa}^* - i C_{M\alpha}^*) \xi - i\phi' \tau \mu + \\ & + (k_t^{-2} C_{Mq}^* + C_D^*) \mu + k_t^{-2} C_{M0}^* e^{i\phi_{M0}} + k_t^{-2} C_{M\delta}^* \delta \end{aligned} \tag{2}$$

where: $C_{L\alpha}$ is the lift force coefficient; ϕ is the roll angle; $C_{Np\alpha}$ is the Magnus force coefficient; $\gamma = \cos(\sqrt{\alpha^2 + \beta})$, being α and β angles of attack and side-slip; k_t is the transverse radius of gyration; C_{Mpa} is the Magnus moment coefficient; $C_{M\alpha}$ is the normal moment slope coefficient; $\tau = 1 - I_x/I_y$, being I_x and I_y axial and transversal moment of inertia; C_{Mq} is the damping moment coefficient; C_D is the drag force coefficient; $C_{M0} e^{i\phi_{M0}}$ is the asymmetric moment coefficient, being C_{M0} the amplitude and ϕ_{M0} the phase; $C_{M\delta}$ is the control moment coefficient; the superscript * means a multiplication by $\rho S d / (2m)$, being S reference area, ρ air density, and m the mass.

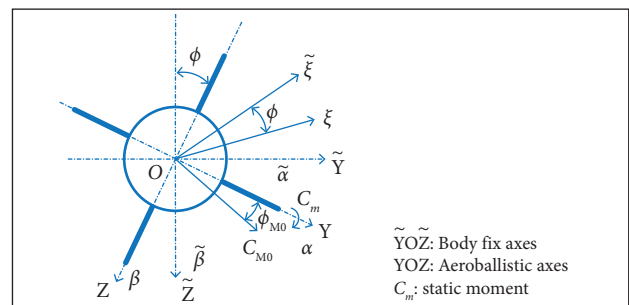


Figure 1. Axes of missile motion.

In Eqs. 1 and 2, ξ' and μ' are the derivatives of ξ and μ with respect to the independent variable l , which has the form $l = d^{-1} \int_0^t V dt$, being V the velocity of the missile, d the reference length and t the time; $\xi = \beta + i\alpha$ is the complex angle of attack in the body fix axes, and $\mu = q + ir$ is the complex angle velocity. $k_t^{-2} C_{M0}^* e^{i\phi_{M0}}$ performs the uncertainty provided by the small asymmetric term. $\delta = \delta + i\delta_y$ is the rudder deflection angle in the yaw and pitch channels.

For rolling missiles, canted fins causing a constant roll moment K_δ are usually used to generate a design steady-state roll rate. Induced roll moment must be taken into account in the rolling motion besides roll moment and roll damping moment. The induced roll moment can be expressed in a simply form varying with α . The roll motion then has the form:

$$\phi'' = -K_p \phi' + K_\delta + K_n \alpha + k_a^{-2} C_{M\delta_r}^* \delta_r \quad (3)$$

where: K_p equals to $-(C_D^* + k_a^{-2} C_{lp}^*)$, being k_a the axial radius of gyration and C_{lp} the roll damping moment; K_δ is the roll moment by canted fins; K_n is the induced roll moment coefficient; $C_{M\delta_r}$ is the rolling control moment coefficient; δ_r is the rudder deflection angle in the roll channel.

When the asymmetric uncertainties are severe, they cannot be simply expressed in a constant. As shown in Fig. 2, when a fin surface is seriously damaged, the uncertainty interference caused by the lost lift dealt as an external force can be approximated as a function of the angle of attack α . Equations 2 and 3 are rewritten into the following forms, respectively:

$$\begin{aligned} & (\phi' C_{M\phi\alpha}^* - i C_{M\alpha}^*) \xi - i \phi' \tau \mu + (k_t^{-2} C_{Mq}^* + C_D^*) \mu + \\ & + k_t^{-2} C_{M0}^* e^{i\phi_{M0}} + k_t^{-2} C_{M\delta}^* \delta + i F_1^* \alpha \end{aligned} \quad (4)$$

$$\phi'' = -K_p \phi' + K_\delta + K_n \alpha + k_a^{-2} C_{M\delta_r}^* \delta_r + F_2^* \alpha \quad (5)$$

where: F_1 and F_2 are the uncertainty force in the angle and roll motion caused by damage.

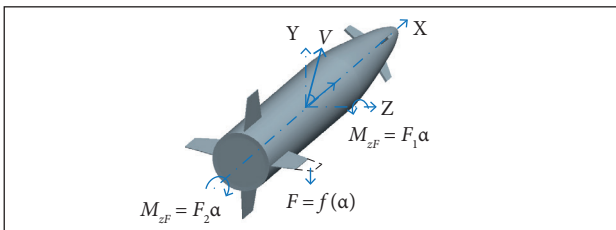


Figure 2. Structural damage schematic diagram.

Thus, Eqs. 1, 4 and 5 constitute the asymmetric rolling missile motion model in three-channel control. Slow loop variables $\Omega = (\beta, \alpha, \phi)^T$ and fast loop variables $\omega = (q, r, p)^T$ are defined, respectively, being $q, r,$ and p yaw, pitch, and roll rates in body fixed axes. Ω responding slowly is the Euler angle vector, and ω responding fast is the angle velocity vector.

According to the time scale separation principle, Eqs. 1, 4 and 5 are rewritten in the forms:

$$\begin{aligned} \begin{pmatrix} \beta \\ \alpha \\ \phi \end{pmatrix}' &= \begin{pmatrix} a_{11} & 0 & 0 \\ 0 & a_{12} & 0 \\ 0 & 0 & a_{13} \end{pmatrix} \begin{pmatrix} \beta \\ \alpha \\ \phi \end{pmatrix} + \begin{pmatrix} 0 & a_{14} & a_{15} \\ a_{16} & 0 & a_{17} \\ 0 & 0 & a_{18} \end{pmatrix} \begin{pmatrix} q \\ r \\ p \end{pmatrix} = \\ &= \begin{pmatrix} f_{11} \\ f_{12} \\ f_{13} \end{pmatrix} + \begin{pmatrix} 0 & a_{14} & a_{15} \\ a_{16} & 0 & a_{17} \\ 0 & 0 & a_{18} \end{pmatrix} \begin{pmatrix} q \\ r \\ p \end{pmatrix} \end{aligned} \quad (6)$$

$$\begin{aligned} \begin{pmatrix} q \\ r \\ p \end{pmatrix}' &= \begin{pmatrix} a_{21}\alpha + a_{23} + a_{25}q + a_{26}pr + a_{28}p\beta \\ -a_{21}\beta + a_{24} + a_{25}r - a_{26}pq + a_{27}\alpha + a_{28}p\alpha \\ a_{41}p + a_{42} + a_{43}\alpha + a_{44}\alpha \end{pmatrix} + \\ &+ \begin{pmatrix} a_{22} & 0 & 0 \\ 0 & a_{22} & 0 \\ 0 & 0 & a_{31} \end{pmatrix} \begin{pmatrix} \delta_y \\ \delta_z \\ \delta_r \end{pmatrix} = \\ &= \begin{pmatrix} f_{21} \\ f_{22} \\ f_{23} \end{pmatrix} + \begin{pmatrix} a_{22} & 0 & 0 \\ 0 & a_{22} & 0 \\ 0 & 0 & a_{31} \end{pmatrix} \begin{pmatrix} \delta_y \\ \delta_z \\ \delta_r \end{pmatrix} \end{aligned} \quad (7)$$

where: $a_{11} = -C_{L\alpha}^*$, $a_{12} = -C_{L\alpha}^*$, $a_{13} = 0$, $a_{14} = -1$, $a_{15} = -(C_{Np\alpha}^* - 1)$, $a_{16} = 1$, $a_{17} = -a_{15}$, $a_{18} = 1$, $a_{21} = k_t^{-2} C_{M\alpha}^*$, $a_{22} = k_t^{-2} C_{M\delta}^*$, $a_{23} = k_t^{-2} C_{M0}^* \cos(\phi_{M0})$, $a_{24} = k_t^{-2} C_{M0}^* \sin(\phi_{M0})$, $a_{25} = k_t^{-2} C_{Mq}^* + C_D^*$, $a_{26} = \tau, -1 - \tau$, $a_{27} = F_1$, $a_{28} = k_t^{-2} C_{Mp\alpha}^*$, $a_{31} = k_t^{-2} C_{M\delta}^*$, $a_{41} = -K_p$, $a_{42} = -K_\delta$, $a_{43} = -K_n$, $a_{44} = F_2$.

TLC PRINCIPLE

As shown in Fig. 3, TLC design method is consisted of two parts. One is forward loop designed by the use of non-linear dynamic inverse method, which changes the trajectory tracking problem into error adjustment problems. Another is state feedback loop designed by the use of linear varying system parallel-differential (PD) spectral theory, which ensures the robustness of the system with model errors. Control model can be represented in two parts as slow and fast loop. The slow

one is missile attitude angles loop, and the fast one is angular velocity loop. The core issue for TLC is the design of gain scheduling control law.

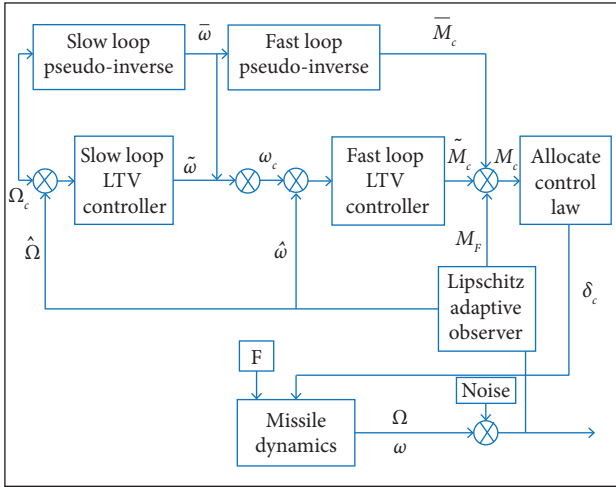


Figure 3. Control system configuration.

NOMINAL CONTROL COMMAND COMPUTING

Let us consider:

$$g_1 = \begin{pmatrix} 0 & a_{14} & a_{15}\alpha \\ a_{16} & 0 & a_{17}\beta \\ 0 & 0 & a_{18} \end{pmatrix}, g_2 = \begin{pmatrix} a_{22} & 0 & 0 \\ 0 & a_{22} & 0 \\ 0 & 0 & a_{31} \end{pmatrix}.$$

Nominal $\bar{\Omega} = \Omega_c$ command of slow loop is the expected control command of missile. Because g_1 is invertible, the nominal command of slow loop is given by:

$$\bar{\omega} = g_1^{-1} (\dot{\bar{\Omega}} - \bar{f}_1) \tag{8}$$

where: $\bar{\omega}$ is also the nominal command of fast loop.

Then the nominal control moment is represented as follows:

$$\bar{M}_c = g_2^{-1} (\dot{\bar{\omega}} - \bar{f}_2) \tag{9}$$

Derivatives $\dot{\bar{\Omega}}$ and $\dot{\bar{\omega}}$ are computed from Ω and ω using a pseudo-differentiator represented by the transfer function:

$$G_{i,diff} = \frac{\omega_{i,diff} S}{s + \omega_{i,diff}}, \quad i = 1, 2 \tag{10}$$

Equation 10 is also a low-pass filter and not only passes through input signal but also avoids output saturation by high-frequency noises.

SLOW LOOP CONTROLLER DESIGN

According to TLC method, linear time-varying proportional-integral (PI) regulator is usually designed to track the augmented vector error. The augmented vector can be expressed as:

$$X_1 = \left[\int \beta dl, \int \alpha dl, \int \phi dl, \beta, \alpha, \phi \right]^T$$

Meanwhile, the slow loop in Eq. 6 can be augmented as:

$$X_1' = \tilde{f}_1(X_1) + \tilde{g}_1(X_1)\omega \tag{11}$$

where: $\tilde{f}_1 = [\beta, \alpha, \phi, f_{11}, f_{12}, f_{13}]^T$ and $\tilde{g}_1 = [O_3 \ g_1^T]^T$, and O_3 is a zero matrix 3×3 .

Equation 11 is linearized in $(\bar{X}_1, \bar{\omega})$. The state and input matrices of the linearized Eq. 11 are represented as:

$$A_1 = \left(\frac{\partial \tilde{f}_1}{\partial X_1} + \frac{\partial \tilde{g}_1}{\partial X_1} \omega \right) \Bigg|_{\bar{X}_1, \bar{\omega}} \tag{12}$$

$$B_1 = \tilde{g}_1 \Big|_{\bar{X}_1, \bar{\omega}} \tag{13}$$

The expected error dynamics characteristic of the slow closed loop is represented as:

$$A_{c1} = \begin{bmatrix} 0 & 0 & 0 & 1 & 0 & 0 \\ 0 & 0 & 0 & 0 & 1 & 0 \\ 0 & 0 & 0 & 0 & 0 & 1 \\ -\alpha_{111} & 0 & 0 & -\alpha_{112} & 0 & 0 \\ 0 & -\alpha_{121} & 0 & 0 & -\alpha_{122} & 0 \\ 0 & 0 & -\alpha_{131} & 0 & 0 & -\alpha_{132} \end{bmatrix} \tag{14}$$

where: $\alpha_{1,jk}, j = 1, 2, 3, k = 1, 2$, varying with time, are obtained from the closed-loop quadratic PD eigenvalues.

The state feedback matrix $K_1(t)$ is deduced from:

$$A_{c1} = A_1(t) + B_1(t)K_1(t) \tag{15}$$

Dynamic error augmented vectors can be defined as:

$$e_{\Omega} = \left[\int (\beta - \bar{\beta}) dl \quad \int (\alpha - \bar{\alpha}) dl \quad \int (\phi - \bar{\phi}) dl \right. \\ \left. \int (\phi - \bar{\phi}) dl \quad \beta - \bar{\beta} \quad \alpha - \bar{\alpha} \quad \phi - \bar{\phi} \right]^T$$

and slow loop control input can be expressed as:

$$\omega_c = \bar{\omega} + K_1(t)e_\omega \tag{16}$$

FAST LOOP CONTROLLER DESIGN

Following the same method to define fast loop dynamics augmented vector error,

$$e_\omega = \left[\int (q - \bar{q}) dt \quad \int (r - \bar{r}) dt \quad \int (p - \bar{p}) dt \quad \int (p - \bar{p}) dt \quad q - \bar{q} \quad r - \bar{r} \quad p - \bar{p} \right]^T$$

augmented equation of fast loop has the form:

$$\dot{X}_2' = \tilde{f}_2(X_2) + \tilde{g}_2(X_2)u \tag{17}$$

The fast loop linearization state matrix and input matrix are provided as:

$$A_2 = \left(\frac{\partial \tilde{f}_2}{\partial X_2} + \frac{\partial \tilde{g}_2}{\partial X_2} u \right) \Big|_{\bar{x}_2, \bar{u}} \tag{18}$$

$$\tilde{g}_2 = \begin{bmatrix} O_3 & g_2^T \end{bmatrix}^T \tag{19}$$

where: $u = [\delta_y \quad \delta_z \quad \delta_r]^T$.

Expected error dynamics characteristic matrix of the fast closed loop can be expressed as follows:

$$A_{c2} = \begin{bmatrix} 0 & 0 & 0 & 1 & 0 & 0 \\ 0 & 0 & 0 & 0 & 1 & 0 \\ 0 & 0 & 0 & 0 & 0 & 1 \\ -\alpha_{211} & 0 & 0 & -\alpha_{212} & 0 & 0 \\ 0 & -\alpha_{221} & 0 & 0 & -\alpha_{222} & 0 \\ 0 & 0 & -\alpha_{231} & 0 & 0 & -\alpha_{232} \end{bmatrix} \tag{20}$$

where: $\alpha_{2,jk}, j = 1, 2, 3, k = 1, 2$, can be given according to PD spectral theory similarly.

State feedback matrix $K_2(t)$ is deduced from the equation:

$$A_{c2} = A_2(t) + B_2(t)K_2(t) \tag{21}$$

The fast loop control input can be expressed as:

$$M_c = \bar{M}_c + K_2(t)e_\omega = \bar{M}_c + \tilde{M}_c \tag{22}$$

LIPSCHITZ ADAPTIVE OBSERVER DESIGN

State observer design is an essential process for a control system, and the compensation control law design is based on

the estimations of state variables and unknown parameters. Lipschitz observer is a common non-linear system state observer and still has a good observation performance for strongly non-linear systems with noise disturbances. Specific design process of Lipschitz observer is characterized as follows (Rajamani 1998; Zemouche and Boutayeb 2013; Pourgholi and Majd 2011).

For a classical non-linear system with unknown parameters:

$$\begin{cases} \dot{x} = Ax + \Phi(x, u) + \Psi(x, u)F \\ y = Cx \end{cases} \tag{23}$$

where: A and C are linear matrices; $x \in \mathbb{R}^n$ is the state vector; $u \in \mathbb{R}^m$ is the control vector; $y \in \mathbb{R}^p$ is the output vector; $F \in \mathbb{R}^l$ is an unknown steady bounded parameter; and $\|F\| \leq \gamma_1$. For all (x, y) and all u the pair (C, A) is observable.

For Eq. 23, make the following three hypotheses (Rajamani 1998; Zemouche and Boutayeb 2013):

Hypothesis (1): non-linear functions $\Phi(x, u)$ and $\Psi(x, u)$ are both uniform boundedness, and $\forall x \in \mathbb{R}^n$ and $\forall u \in \mathbb{R}^m$, Lipschitz condition is satisfied as follows:

$$\begin{cases} \|\Phi(x_1, u) - \Phi(x_2, u)\|_2 \leq \gamma_2 \|x_1 - x_2\|_2 \\ \|\Psi(x_1, u) - \Psi(x_2, u)\|_2 \leq \gamma_3 \|x_1 - x_2\|_2 \end{cases} \tag{24}$$

where: $\gamma_2 > 0$ and $\gamma_3 > 0$ are Lipschitz constants.

Hypothesis (2): there exist a gain matrix and a positive number ε making algebraic Riccati equation:

$$(A - LC)^T P + P(A - LC) + \gamma PP + (1 + \varepsilon)I = 0 \tag{25}$$

have a positive definite solution P , where $\gamma = \gamma_2 + \gamma_1 \gamma_3$.

Hypothesis (3): there exists a vector function $h(x, u)$ making the positive definite solution P satisfy:

$$P\Psi(x, u) = C^T h(x, u) \tag{26}$$

If the Hypotheses (1) to (3) conditions are satisfied, then the observer of the Eq. 23 is given as follows:

$$\begin{cases} \dot{\hat{x}} = A\hat{x} + \Phi(\hat{x}, u) + \Psi(\hat{x}, u)\hat{F} - L(y - C\hat{x}) \\ \dot{\hat{F}} = \rho h^T(\hat{x}, u)(y - C\hat{x}) \end{cases} \tag{27}$$

where: ρ is a constant parameter to adjust the estimation error and $\hat{F} = [\hat{F}_1, \hat{F}_2]$. L is the gain matrix of the observer.

L is obtained by transforming Riccati equation into the linear matrix inequality (LMI) problem (Pourgholi and Majd 2011).

In this paper, according to the Lyapunov stability conditions, the design of observer is changed to the process of solving LMI group.

LMI problem is equivalent to find a definite solution $P > 0$ and a positive number $\eta > 0$ satisfies the inequality equation:

$$\begin{bmatrix} A^T P + PA - 2\eta C^T C + I & P \\ P & -\frac{1}{\gamma^2} I \end{bmatrix} < 0 \tag{28}$$

By solving the above inequality (Eq. 28), L can be obtained as:

$$L = \eta P^{-1} C^T \tag{29}$$

COMPENSATION CONTROL LAW DESIGN

Compensation control law is given according to the estimated parameter \hat{F} . The control law can compensate for the interference generated by the F in the pitch and roll channels, and then TLC control performance is improved. Furthermore, in order to improve the yaw channel performance, the state feedback stabilization is increased. Compensation control law is shown as follows:

$$M_F = \begin{bmatrix} -K_\beta \hat{\beta} / a_{22} & -\hat{F}_1 \hat{\alpha} / a_{22} & -\hat{F}_2 \hat{\alpha} / a_{31} \end{bmatrix}^T \tag{30}$$

where: K_β is the adjusting gain.

The improved TLC control law based on Lipschitz adaptive compensation is then proposed as:

$$M_c = \bar{M}_c + \tilde{M}_c + M_F \tag{31}$$

SIMULATION

Simulation analysis for an asymmetric rolling missile is performed, and system parameters are:

$$\begin{aligned} a_{11} &= -2.3 \times 10^{-4}, a_{12} = -2.3 \times 10^{-4}, a_{13} = 1, a_{15} = 1, a_{21} = -1.4 \times 10^{-5}, \\ a_{22} &= 1 \times 10^{-5}, a_{23} = -2.4947 \times 10^{-7}, a_{24} = 2.4947 \times 10^{-7}, a_{25} = -1.5 \times 10^{-4}, \\ a_{26} &= 0.99, a_{28} = -1 \times 10^{-5}, a_{31} = 9 \times 10^{-4}, a_{41} = -1.3 \times 10^{-3}, \\ a_{42} &= 5 \times 10^{-6}, a_{43} = 5.2 \times 10^{-4}, F_1 = 0, F_2 = 0. \end{aligned}$$

SIMULATION 1

Equations 6 and 7 can be easily transformed into a standard non-linear form with unknown parameter as Eq. 23. In order to verify the state observation and the noise suppressing performance of Lipschitz state observer, external forces F_1 and F_2 are taken to 0. In addition, system state observations often

have some uncertainty. For example, the output values of the measurement system are usually superimposed with white noise. In order to represent the sensor noise, the output values are superimposed on white noise in simulation. Meanwhile, the actual value of the aerodynamic parameters increases by 20% compared with the estimated one.

The expected tracking states “command” in yaw, pitch and roll channels are β_c , α_c and p_c , respectively. It means that the motion states β , α and p of the missile are expected to change as the commands β_c , α_c and p_c require, as shown in Fig. 3. The specific command for β_c in yaw channel is a square wave; the specific command for α_c in pitch channel is a step response; and the specific command for p_c in roll channel is a constant. These three commands are all passed through a low-pass filter $5s/(s + 5)$.

According to Eq. 29, let us take the gain matrix L as:

$$L = \begin{pmatrix} 4.25 & 0 & 0 & 0 & -1.90 & 0 \\ 0 & 4.31 & -0.02 & 1.70 & 0 & -2.15 \\ 0 & -0.02 & 5.49 & -0.46 & 0 & -2.33 \\ 0 & 1.70 & -0.46 & 548.21 & 0 & -504.29 \\ -1.90 & 0 & 0 & 0 & 589.88 & 0 \\ 0 & -2.15 & -2.33 & -504.29 & 0 & 483.77 \end{pmatrix}$$

The simulation results are shown in Figs. 4 to 6. The expected motion states in the three channels of β , α and p are meant to track the commands β_c , α_c and p_c which are marked in black line. To track the same commands β_c , α_c and p_c , different control effectiveness in TLC method and “TLC + Lipschitz observer” method is compared. The control effectiveness of TLC method is marked in blue dash line, and the control effectiveness of “TLC + Lipschitz observer” is marked in red line. As shown in Figs. 4 to 6, in the case of aerodynamic parameters deviation and output noise conditions, control accuracy of only TLC method is poor, and there exist large errors. When Lipschitz state

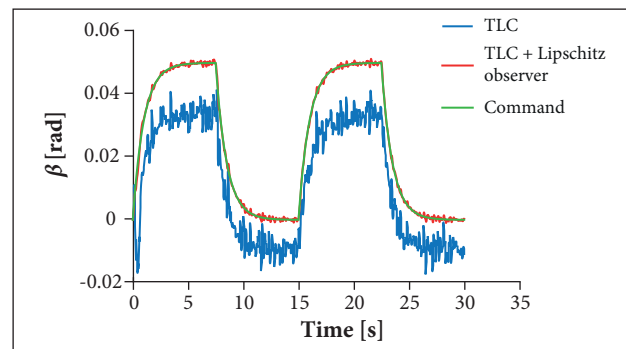


Figure 4. Effectiveness of yaw control.

observer is used, noise is effectively suppressed. It is apparent that the controller has good tracking performance even with output noise interference.

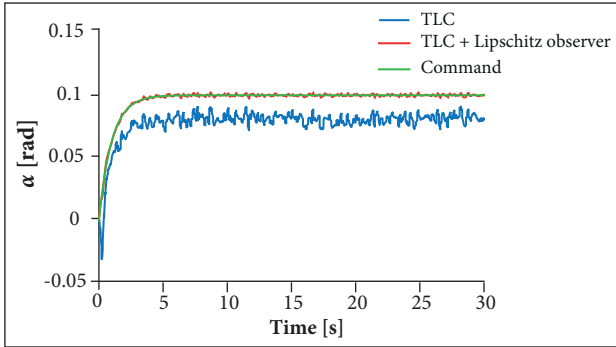


Figure 5. Effectiveness of pitch control.

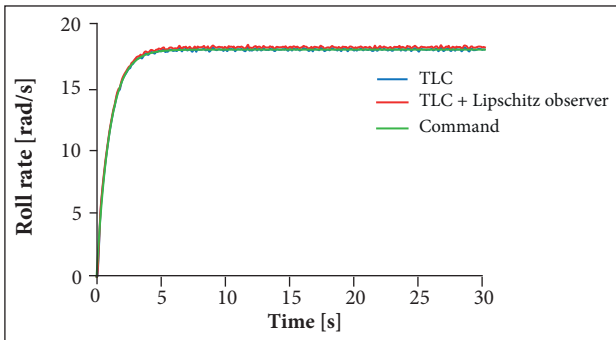


Figure 6. Effectiveness of roll control.

SIMULATION 2

To verify the estimate effectiveness of Lipschitz adaptive observer, let us consider $F_1 = 100$ and $F_2 = 200$; the state variables for the missile in the free movement are estimated, as shown in Figs. 7 to 10. Simulation results show that state observer can estimate the state variables and unknown parameters quickly and accurately.

Another simulation is performed to verify the performance of the improved TLC method. In addition, structural damage for missiles often happens suddenly, and it is supposed that a fin of the missile is suddenly damaged on 5s after the beginning of the simulation. The damage effectiveness is $F_1 = 100$ and $F_2 = 200$. At the same time, the actual value of aerodynamic parameters is reduced 25% compared to the estimated value, and the simulation results are shown in Figs. 11 to 14.

The specific command for β_c in yaw channel and α_c in pitch channel is a step response signal, and the specific command for p_c in roll channel is a constant. These three commands are all passed through a low-pass filter $5s/(s + 5)$. In the figures, the expected attitudes which are named “command” are marked

in black line. Two different methods “TLC” and improved TLC which is named “TLC + adaptive compensation” are separately applied to control the missile attitudes to track the “command”.

The figures show that an only algorithm using TLC has certain robustness in dealing with the uncertainties of aerodynamic parameters. However, the control effectiveness is not ideal in response to a sudden but strong interference, and even the system is going to diverge. “TLC” cannot match “command” in a good performance. The figures exhibit a perfect match between “command” and “TLC + adaptive compensation”. It means that TLC combined with Lipschitz adaptive compensation control law improves the

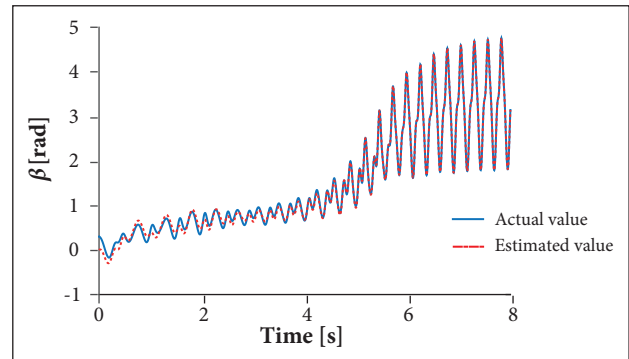


Figure 7. Actual and estimated β .

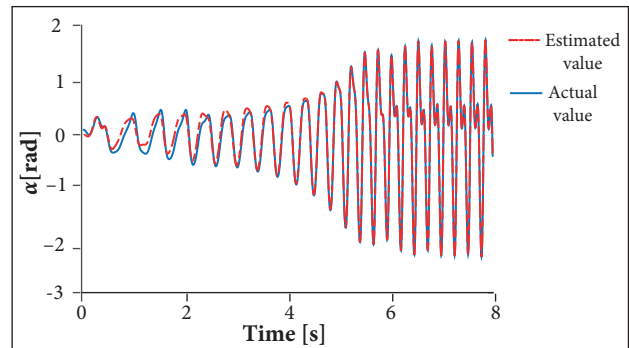


Figure 8. Actual and estimated α .

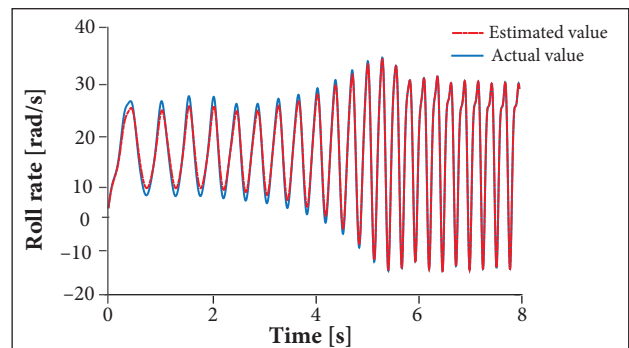


Figure 9. Actual and estimated p .

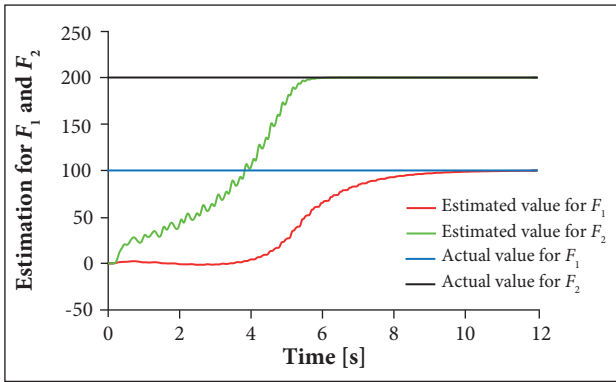


Figure 10. Actual and estimated F .

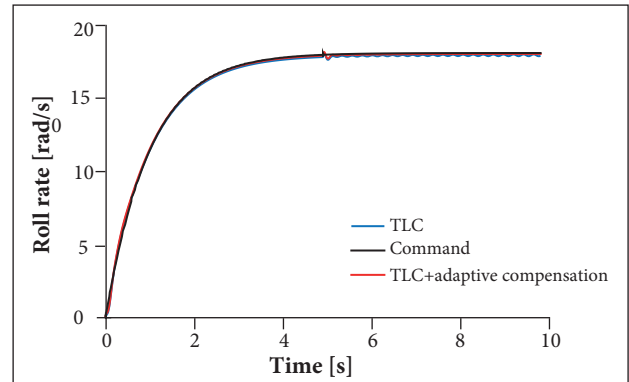


Figure 13. Effectiveness of roll control.

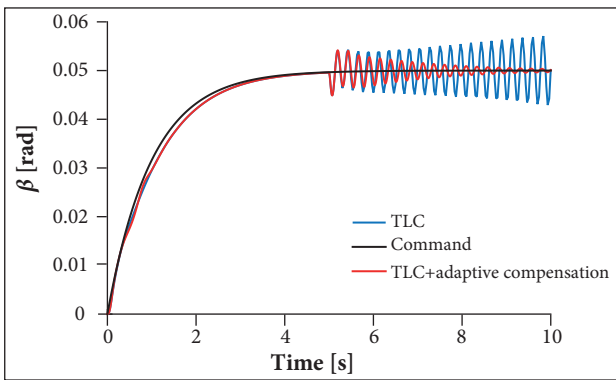


Figure 11. Effectiveness of yaw control.

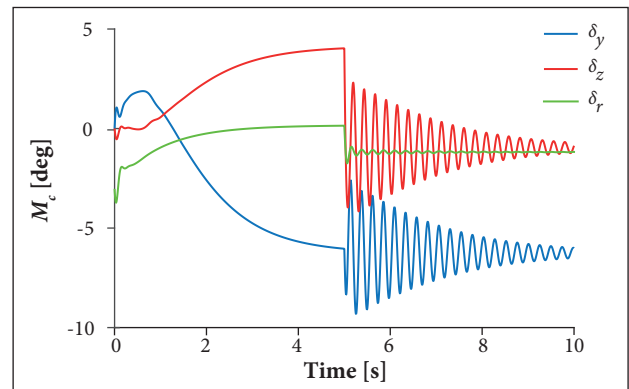


Figure 14. Rudder deflection angles for three-channel control in "TLC + adaptive compensation".

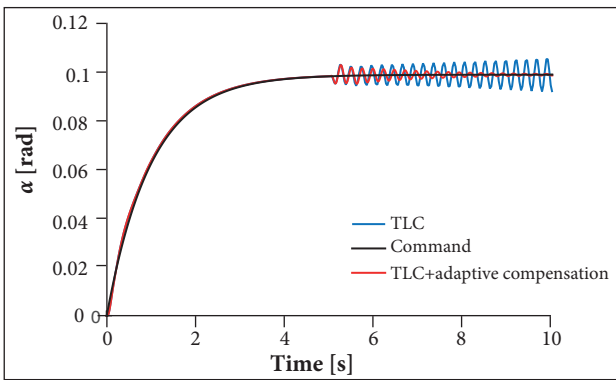


Figure 12. Effectiveness of pitch control.

control performance in three channels and enhances the robustness of the system. The missile system can converge to the expected state of motion more accurately and quickly with strong external interference. The adaptive decoupling control solves the cross coupling in three channels. The rudder deflection angles of TLC method are lead to saturation when control system diverges, and then TLC method becomes invalid. Compared to TLC, the rudder deflection angles of improved TLC are easy to achieve without saturation

phenomenon, and this means that the improved TLC method is physically realizable.

CONCLUSIONS

In this paper, the non-linear control method for asymmetric rolling missiles is investigated. Firstly, an asymmetric rolling missile controlled motion model is established considering inherent asymmetric aerodynamic force and damage fin uncertain external interference. Then, a preliminary controller is presented by the TLC method in the time-scale separation principle. Thirdly, an improved TLC method with adaptive compensation control law based on Lipschitz observer is proposed. In the improved method, the classic TLC method is complementary by an adaptive compensation control law, and this is designed according to the estimated unknown parameters and state variables from Lipschitz observer. Finally, control effectiveness comparison of TLC and improved TLC is carried out by simulation, and adaptive decoupling control for three channels is achieved.

Simulation results demonstrate that improved TLC is more effective than classic TLC method, and the proposed improved TLC method exhibits a good performance in the track ability, robustness and adaptability.

ACKNOWLEDGEMENT

This study was supported by the National Natural Science Foundation of China (No. 11532002).

REFERENCES

- Ananthkrishnan N, Raisinghani SC (1992) Steady and quasisteady resonant lock-in of finned projectiles. *J Spacecraft Rockets* 29(5):692-696. doi: 10.2514/3.11512
- Bevacqua T, Best E, Huizenga A, Cooper D, Zhu JJ (2004) Improved trajectory linearization flight controller for reusable launch vehicles. Proceedings of the 42nd AIAA Aerospace Sciences Meeting and Exhibit; Reno, USA.
- Djellal S, Ouibrahim A (2008) Aerodynamic performances of battle-damaged and repaired wings of an aircraft model. *J Aircraft* 45(6):2009-2023.
- Harris J, Slegers N (2009) Performance of a fire-and-forget anti-tank missile with a damaged wing. *Math Comput Model* 50(1-2):292-305. doi: 10.1016/j.mcm.2009.02.009
- Liu Y, Wu X, Zhu JJ, Lew J (2003) Omni-directional mobile robot controller design by trajectory linearization. Proceedings of the 2003 American Control Conference; Denver, USA.
- Mickle MC, Zhu JJ (2001) Skid to turn control of the APKWS missile using trajectory linearization technique. Proceedings of the 2001 American Control Conference; Arlington, USA.
- Mikhail AG (1998) Fin damage and mass offset for kinetic energy projectile spin/pitch lock-in. *J Spacecraft Rockets* 35(3):287-295. doi: 10.2514/2.3353
- Morote J (2007) Analytic model of catastrophic yaw. *J Spacecraft Rockets* 44(5):1029-1037. doi: 10.2514/1.29858
- Morote J, Garcia-Ybarra PL, Castillo JL (2013) Large amplitude oscillations of cruciform tailed missiles. Part 1: catastrophic yaw fundamental analysis. *Aero Sci Tech* 25(1):145-151. doi: 10.1016/j.ast.2012.01.002
- Murphy CH (1963) Free flight motion of symmetric missiles. BRL Report No. 1216. Aberdeen Proving Ground: U. S. Army Ballistic Research Laboratory. AD 442757.
- Murphy CH (1989) Some special cases of spin-yaw lock-in. *J Guid Control Dynam* 12(6):771-776. doi: 10.2514/3.20480
- Nguyen N, Krishnakumar K, Kaneshige J (2006) Dynamics and adaptive control for stability recovery of damaged asymmetric aircraft. Proceedings of the AIAA Guidance, Navigation, and Control Conference and Exhibit; Keystone, USA.
- Pourgholi M, Majd VJ (2011) A nonlinear adaptive resilient observer design for a class of Lipschitz systems using LMI. *Circ Syst Signal Process* 30(6):1401-1415. doi: 10.1007/s00034-011-9320-y
- Rajagopal K, Balakrishnan SN, Nguyen N, Krishnakumar K (2010) Robust adaptive control of a structurally damaged aircraft. Proceedings of the AIAA Guidance, Navigation, and Control Conference; Toronto, Canada.
- Rajamani R (1998) Observers for Lipschitz nonlinear systems. *IEEE Trans Automat Contr* 43(3):397-401. doi: 10.1109/9.661604
- Render PM, De Silva S, Walton A, Mani M (2007) Experimental investigation into the aerodynamics of battle damaged airfoils. *J Aircraft* 44(2):539-549. doi: 10.2514/1.24144
- Render PM, Samaad-Suhaeb M, Yang Z, Mani M (2009) Aerodynamics of battle-damaged finite-aspect-ratio wings. *J Aircraft* 46(3):997-1004. doi: 10.2514/1.39839
- Su XL, Yu JQ, Wang YF, Wang LL (2013) Moving mass actuated reentry vehicle control based on trajectory linearization. *International Journal of Aeronautical and Space Sciences* 14(3):247-255. doi: 10.5139/UASS.2013.14.3.247
- Sun H, Yu J, Zhang S (2015) Bifurcation analysis of the asymmetric rolling missiles. *Proc IME G J Aero Eng* 26(9):1-2. doi: 10.1177/0954410015606941
- Tanrkulu O (1999) Limit cycle and chaotic behavior in persistent resonance of unguided missiles. *J Spacecraft Rockets* 36(6):859-865. doi: 10.2514/2.3504
- Yang I, Kim D, Lee D (2012) A flight control strategy using robust dynamic inversion based on sliding mode control. Proceedings of the AIAA Guidance, Navigation, and Control Conference; Minneapolis, USA.
- Zemouche A, Boutayeb M (2013) On LMI conditions to design observers for Lipschitz nonlinear systems. *Automatica* 49(2):585-591. doi: 10.1016/j.automatica.2012.11.029
- Zhu JJ, Huizenga AB (2004) A type two linearization controller for a reusable launch vehicle — a singular perturbation approach. Proceedings of the AIAA Atmospheric Flight Mechanics Conference and Exhibit; Providence, USA.